Progress In Electromagnetics Research Letters, Vol. 108, 85–92, 2023

Circularly Polarized Conformal Antenna with Dual V-Shaped Coupling Feed Lines

Zhengkun Yang[1], Na Kou[2, *], Shixing Yu[2], and Jubo Guo[1, 2]

Abstract—A wideband, compact, and flexible conformal circularly polarized antenna (CCPA) with ground plane is proposed in this letter. It consists of a polygonal patch, two V-shaped coupling feed lines, a phase-shift transmission line, and two layers of metallic ground planes. Two resonant modes are generated by cutting one vertex of the octagonal patch to broaden the operational bandwidth. An L-shaped ground plane is designed on the back of the top substrate. This configuration can obtain a relatively compact phase shifter on the one hand and make the coupling branches and octagonal patch share one ground plane on the bottom, improving the thickness of the antenna which yields wide bandwidth on the other hand. The CCPA can own good performances both in the planar and cylindrical carriers. Under the cylindrical conformal circumstance, the measured $|S_{11}|$ and axial ratio (AR) bandwidth reach 12.05% (5.5 GHz–6.205 GHz) and 8.93% (5.67 GHz–6.2 GHz), respectively. The measured gain is 8.5 dBic with 3 dB gain bandwidth covering the whole operational band.

1. INTRODUCTION

Circularly polarized (CP) antenna plays an important role in modern wireless communication systems. They have been widely applied in practice due to the inhibition of multipath effects and adaptability to harsh environments. In recent years, antennas have been hidden through various technologies to adapt to the development of modern wireless communication devices. In an outdoor environment, the antenna is required to be hidden on the carrier without destroying the appearance of the carrier. It is well known that conformal antennas can integrate with various wireless communication systems without damaging their physical appearance and aerodynamic features. Hence, the combination of conformal antenna and circularly polarized one can yield great potential applications, such as Internet of Things (IoT). Conformal circularly polarized antennas (CCPAs) have been widely adopted on conductive surfaces such as drones [1], cars [2], or telegraph poles [3] in IoT devices.

Most of the conformal CP array antennas are based on traditional patch antennas which own narrow bandwidths and low efficiencies. Therefore, these antenna elements need to form a large-scale array to achieve high gain feature [4, 5]. Some wide band CCPAs can directly integrate with the carriers [6, 7]. The size of these antennas, however, is too large for modern IoT devices. Some compact conformal antennas with coplanar waveguide feeding (CPW) achieve good performances, but they lack ground plane which causes high back radiations [8, 9], thus cannot be applied in conductive surfaces. Therefore, the study on high-performance CCPAs with compact size and wide operational bandwidth for conductive surfaces is urgent.

Most of the researches aim at solving the big size or narrow CP operating bandwidth problems [10–12]. But these designs cannot be applied in conformal surfaces because they have no flexible substrates.

Received 29 October 2022, Accepted 14 December 2022, Scheduled 4 January 2023

* Corresponding author: Na Kou (nkou@gzu.edu.cn).

[1] Jiangnan Design and Research Institute of Machinery and Electricity, Guiyang, Guizhou 550009, China. [2] College of Big Data and Information Engineering, Guizhou University, Guiyang, Guizhou 550025, China.

Quite a few works use flexible materials such as polyethylene glycol terephthalate (PET) or foam to design the conformal antennas. However, they are vulnerable to damage and of high cost.

In this letter, a broadband, compact, and flexible CCPA with ground planes is proposed. It adopts two layers of ultra-thin F4B substrates which are flexible for conformal application. Two V-shaped coupling branches are designed to feed the polygonal patch with a cut corner which generates two orthogonal modes, thus broadening the operational bandwidth. An L-shaped ground plane is designed on the back of the top substrate, achieving a relatively compact phase shifter and improving the thickness between the ground plane on the bottom and the radiation patch which yields wide working bandwidth. Measured results show that the CCPA achieves a wide impedance and axial ratio (AR) bandwidth. It also owns good adaptability to the cylindrical carrier with radius of 50 mm. In addition, the backside electromagnetic interference can be eliminated due to the metal ground plane, so the proposed antenna can be widely used for IoT devices and mobile carriers with conductive surfaces.

2. ANTENNA DESIGN

2.1. Antenna Configuration

Figure 1 shows the geometry and size of the proposed antenna (unit: mm). It consists of two dielectric substrates which are connected by copper pillars. The radiation structure on the top is a polygonal patch with a cut corner, which can generate two resonant modes to improve the bandwidth. Two V-shaped coupling feed lines are designed for impedance matching. In addition, a 90° phase-shift transmission line is connected to the V-shaped coupling lines to produce the required phase difference for generating circular polarization. An L-shaped metallic plane (ground-1) is designed as the ground of the phase shifter. The reason that we choose two layers of ground planes is that it can greatly reduce the size of feeding lines in order to minimize its effect on radiation structure. It is worth mentioning that the length of the substrate-2 ($L_b = 37.13$ mm) is slightly smaller than the substrate-1 ($L = 41.2$ mm) for easy installation of SMA (Sub Miniature version A) connector. The two substrates own dielectric constant of $\varepsilon_r = 2.65$, loss tangent of $\tan\delta = 0.002$, and thickness of $h = 0.254$ mm. The ultra-thin substrates facilitate conformal application of the antenna on cylindrical surface.

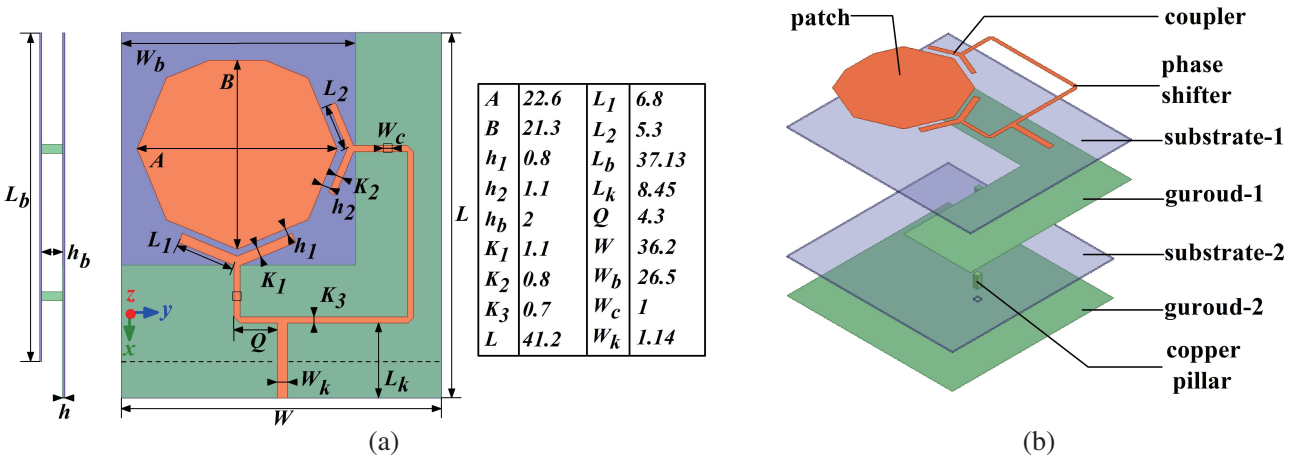

A	22.6	L_1	6.8
B	21.3	L_2	5.3
h_1	0.8	L_b	37.13
h_2	1.1	L_k	8.45
h_b	2	Q	4.3
K_1	1.1	W	36.2
K_2	0.8	W_b	26.5
K_3	0.7	W_c	1
L	41.2	W_k	1.14

Figure 1. Geometry of the proposed antenna: (a) the top view, (b) the perspective view.

2.2. Operating Principle

When a regular octagonal patch is fed by a V-shaped coupling line, the surface current is shown in Figure 2(a). The vertical currents (shown by black arrow) are generated, and the antenna operates at 5.8 GHz with a narrow bandwidth, as shown in Figure 2(b). Next, two perpendicular V-shaped coupling feed lines are introduced for generating two orthogonal E-field components, as shown in Figure 2(c).

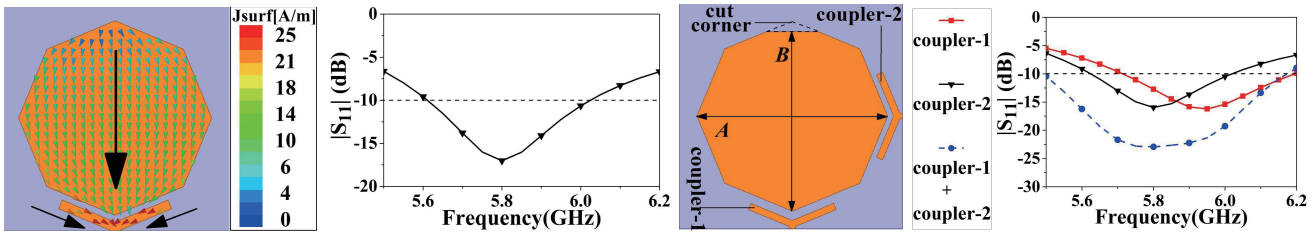

Figure 2. (a) Current distribution and (b) $|S_{11}|$ of the octagon patch antenna. (c) Geometry and (d) $|S_{11}|$ of the octagon antenna with a cut corner fed by two perpendicular V-shaped coupling lines.

The amplitudes of the two E-field components can be controlled by the means of changing the resonant frequency of the mode. The electric length A or B controls the center resonant frequency of each orthogonal mode, which in turn can adjust the amplitudes of the two E-filed components. The larger the electrical length is, the lower the resonant frequency can be generated. To broaden the operational bandwidth, we cut a corner of the octagonal patch which can make the equivalent electrical lengths of the patch become unequal in the vertical and horizontal directions. As a result, feeding by coupler-1 can produce a resonant mode at 5.8 GHz, while feeding by coupler-2 can generate a resonant mode at 5.95 GHz which is shown in Figure 2(d). When the two V-shaped coupling lines are connected, the two resonant modes can be combined to generate a wide operational bandwidth, as shown in Figure 2(d).

Since generating circular polarization requires that the phase difference between two orthogonal E-field components reaches 90° while the amplitudes of the two components are equal, a 90° phase-shift transmission line is added which corresponds to ground-1 on the back of substrate-1, as shown in Figure 3(a). To expand the CCPA's operational bandwidth, copper pillars were added, which not only increased the distance between the radiant patch and ground-2, but also connected ground-1 to ground-2.

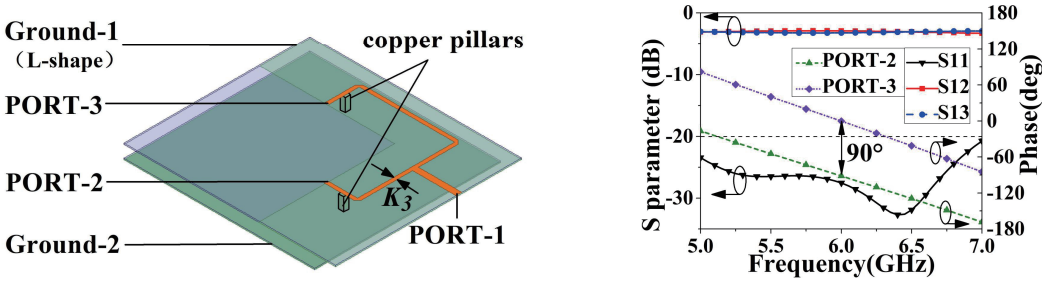

Figure 3. (a) The structure and (b) S-parameters of the 90° phase-shift transmission line.

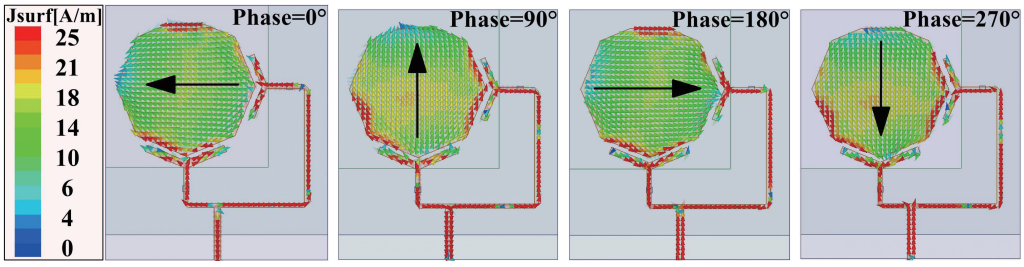

Figure 4. Surface current of (a) 0°, (b) 90°, (c) 180° and (d) 270° phase at 5.8 GHz.

As aforementioned, the L-shaped ground plane is designed for reducing the size of the transmission line, and it also avoids blocking the radiated patch. Figure 3(b) shows that the feed network operates from 5 GHz to 7 GHz when $|S_{11}|$ is below -20 dB, and $|S_{12}|$ and $|S_{13}|$ are both around -3 dB. Furthermore, the phase difference between port-2 and port-3 remains stable at 90° across 5 GHz to 7 GHz.

The black arrows in Figure 4 show the directions of surface current when different input phases are excited at 5.8 GHz. The horizontal currents can be generated when input phases are 0° and 180°, and the currents under 90° and 270° input phases are vertical. From Figure 4 we can see that the two E-field components generated by the two V-shaped coupling lines have almost equal amplitude.

2.3. Numerical analysis for the antenna

Firstly, the distances between the radiated patch and the two V-shaped coupling lines (h_1 and h_2 shown in Figure 1(a)) affect the impedance matching because they can change the coupling strength between radiation patch and coupling line. Taking coupler-1 as an example, we can see from Figures 5(a) and (b) that the antenna achieves a relatively ideal circular polarization when h_1 is around 0.8 mm. When h_1 is reduced, the coupling strength at the upper band increases, and the value of $|S_{11}|$ varies from -33 dB to -23 dB in the low band. The amplitude of the E-field component generated by feeding coupler-1 also increases, which further affects the AR performance, as shown in Figure 5(b). In addition, through the research, we find that L_1 and L_2 have similar effects on coupling strength as h_1.

In the geometry of the CCPA, h_b is the distance between ground-1 and ground-2. Figure 6(a) indicates that when h_b increases, impedance bandwidth is broadened. Meanwhile, h_b can also significantly affects the location of the AR bandwidth, as shown in Figure 6(b).

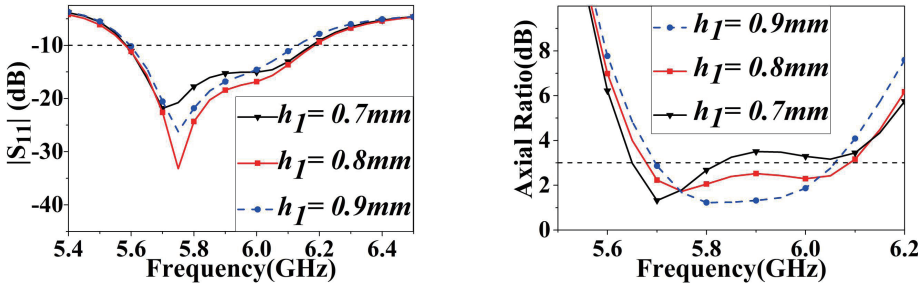

Figure 5. Simulated (a) $|S_{11}|$ and (b) AR of the proposed antenna with different h_1.

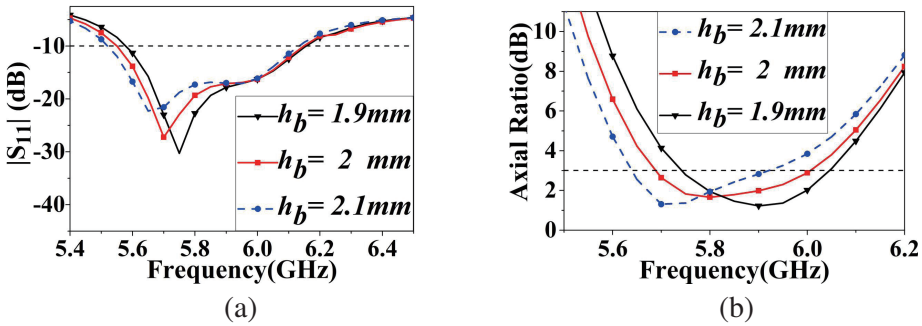

Figure 6. Simulated (a) $|S_{11}|$ and (b) AR of the proposed antenna with different h_b.

3. EXPERIMENTAL VERIFICATION

Figure 7(a) shows the fabricated prototypes of CCPA under cylindrical and planar surfaces. The thickness of traditional low-profile antennas is about 1 mm–3 mm in C-band, which is inflexible for

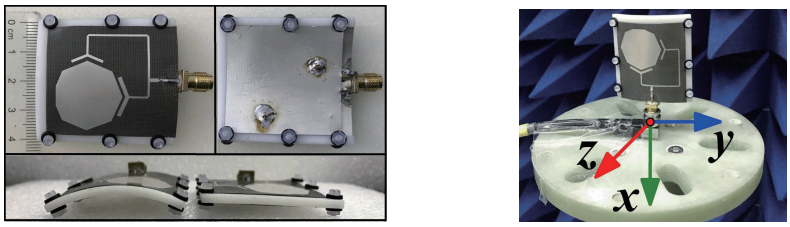

(a) (b)

Figure 7. (a) The fabricated prototype of antenna and (b) its measurement configuration in the coordinate (x-y-z axes) system.

conformal surfaces. However, reducing the thickness of the antenna would significantly deteriorate its operational bandwidth. Therefore, two layers of substrates, each with the thickness of 0.254 mm, are utilized to better conform to the curved surface. The air layer is also adopted to improve the operational bandwidth. The fabricated antenna is installed on the supports made by 3D printing technology. The fabricated antenna is installed on a hollow support made of 3D printing technology, which forms an air gap between the two layers of substrates to expand the operation bandwidth. In addition, the measurement configuration is shown in Figure 7(b).

Figure 8 shows that when the radius of the carrier is reduced from 55 mm to 50 mm, the simulated $|S_{11}|$ and AR bandwidth of the conformal antenna remain unchanged. However, when the radius is reduced to 45 mm, the AR bandwidth of the antenna is significantly deteriorated. Therefore, the minimum cylindrical carrier radius that the antenna can accommodate is $R = 50$ mm. The CCPAs under planar and cylindrical supports are measured respectively. The simulated and measured results agree well with each other. We can see from Figure 8(a) that the measured bandwidth of CCPA with planar support ranges from 5.56 GHz to 6.23 GHz with relative bandwidth of 11.37% ($|S_{11}|$ is below -10 dB). When the CCPA is placed on a cylindrical support with radius of 50 mm, the working frequency covers 5.5 GHz–6.205 GHz with relative bandwidth of 12.05%. The 3-dB AR relative bandwidth of the CCPA under planar and cylindrical supports reaches 7.13% (5.68 GHz–6.1 GHz) and 8.93% (5.67 GHz–6.2 GHz), respectively, as shown in Figure 8(b). Since h_b becomes larger in measurement due to the thickness error of the 3D printing frame, the measured AR bandwidth is slightly wider than the simulated one.

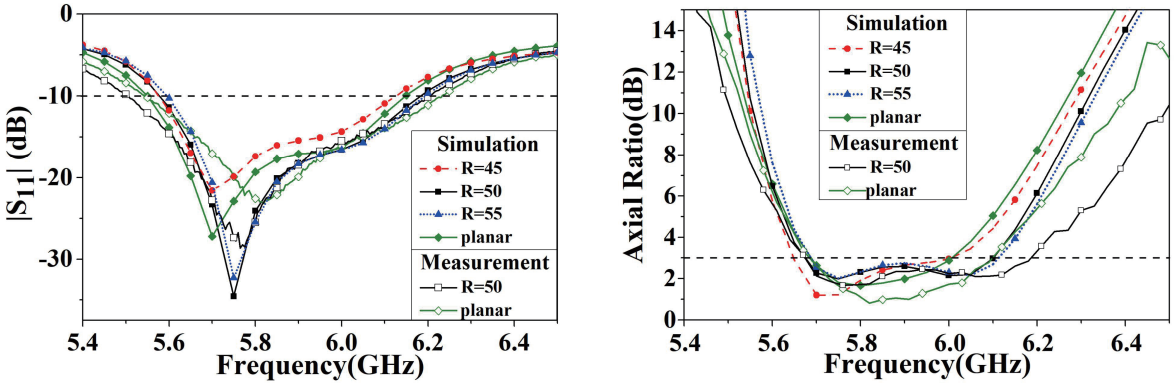

(a) (b)

Figure 8. Comparison of (a) $|S_{11}|$ and (b) AR of the antenna between simulation and measurement.

Figure 9 shows simulated and measured gains of the CCPA under cylindrical and planar supports. We can see that the gain of CCPA under cylindrical conformal condition reaches at least 6 dBic in the operational frequency range, and the highest gain value is 8.5 dBic at 5.96 GHz. The measured gain of the antenna under planar case reaches above 7.5 dBic in operational band, and the peak gain reaches

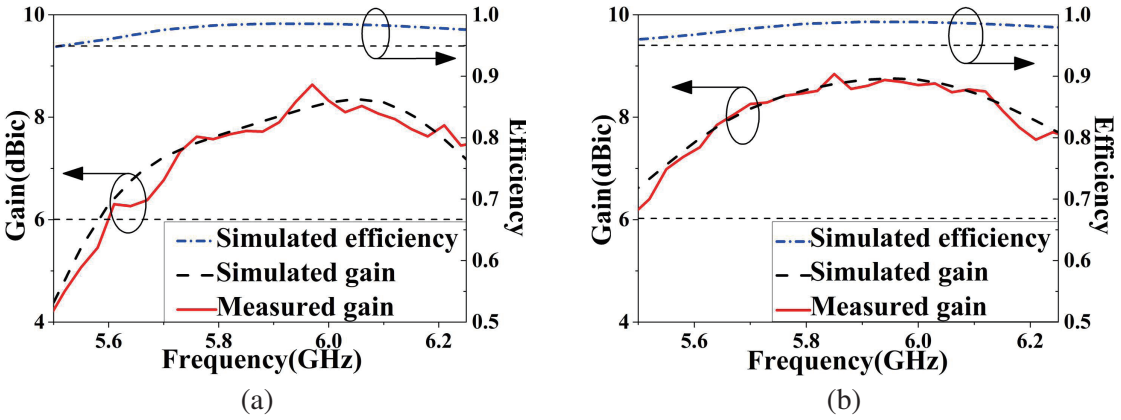

Figure 9. Simulated and measured gain and simulated efficiency of the proposed antenna on the (a) cylindrical conformal condition and (b) planar condition.

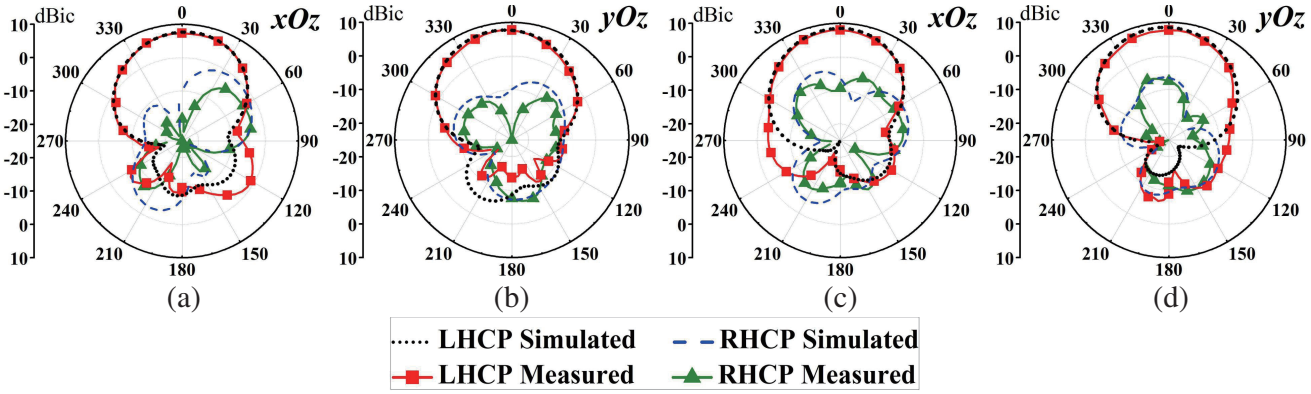

Figure 10. Simulated and measured radiation patterns of the conformal antenna with the cylinder radius=50 mm. (a)–(b) 5.8 GHz, (c)–(d) 6.1 GHz.

Table 1. Performance comparison.

Ref.	Type	Electrical Size (λ_0^3)	CP bandwidth (GHz, %)	Eff. (%)	Gain (dBic)
[4]	Conformal $2*10$ array	$4.9*0.28*0.02$	9.5–9.9, 4.1	-	10.5
[5]	Conformal $4*4$ array	$2.8*2.8*0.05$	7.7–8.3, 8.6	71	15.4
[10]	Planar unit	$0.38*0.38*0.024$	1.61–1.63, 1.5 2.47–2.5, 1.	- -	3.3 4.2
[11]	Planar unit	$0.96*0.96*0.028$	3.8–4.15, 8.8	95	5.8
[12]	Planar unit	$0.88*0.88*0.042$	4.76–5.1, 7.07	-	3.5
This work	Planar unit Conformal unit	$0.75*0.66*0.046$	5.68–6.1, 7.13 5.67–6.2, 8.93	98 97	8.7 8.5

8.7 dBic at 5.84 GHz. Figure 9 also shows the simulated radiation efficiency of the antenna under the two conditions which both reach above 95%.

Finally, the simulated and measured radiation patterns of the conformal antenna at 5.8 GHz and 6.1 GHz are compared in Figure 10. We can see that the two results agree well with each other. When

the CCPA is conformed to the cylindrical surface with the radius of 50 mm, it radiates left-hand circular polarization (LHCP) wave in the normal direction. In addition, since we add a metal ground on the back, the cross-polarization level is lower than −10 dBic. Therefore, the backside electromagnetic interference can be eliminated in conformal applications especially when the platform is of metal curved surfaces.

Table 1 shows the performance comparison between the proposed antenna and related CP antennas. We can see that the CCPA proposed in this paper can obtain a relatively wide bandwidth under conformal condition, and the gain of the antenna element is higher than other designs. In addition, the proposed antenna is also of simple structure, low profile, and low cost, which can be widely applied to conformal platforms in the future.

4. CONCLUSIONS

A conformal circularly polarized antenna with V-shaped coupling branches is proposed. By introducing an L-shaped ground, the phase-shift line is miniaturized. The impedance matching can be simplified by a symmetrical coupling feed structure. The CP bandwidths of the conformal and planar antenna reach 8.93% and 7.13%, and the peak gains of 8.5 dBic and 8.7 dBic can be achieved, respectively. Compared with other similar antennas, it has the advantages of wide CP bandwidth, high gain, and low cost. The proposed antenna can be applied to the wireless communication systems operating at WLAN (5.8 GHz) or part of the C-band (4 GHz–8 GHz), and it owns good adaptability to conformal platforms, which can be widely used for IoT devices or mobile carriers with conductive surfaces.

REFERENCES

1. Santosa, C. E. and J. T. S. Sumantyo, "Conformal subarray antenna for circularly polarized synthetic aperture radar onboard UAV," *2020 International Symposium on Antennas and Propagation (ISAP)*, 5–6, 2021.
2. Mingo, J., C. Roncal, and P. L. Carro, "3-D conformal spiral antenna on elliptical cylinder surfaces for automotive applications," *IEEE Antennas and Wireless Propagation Letters*, Vol. 11, 148–151, 2021.
3. Zhao, Y., Z. Shen, and W. Wu, "Conformal SIW H-plane horn antenna on a conducting cylinder," *IEEE Antennas and Wireless Propagation Letters*, Vol. 14, 1271–1274, 2015.
4. Ogurtsov, S. and S. Koziel, "A conformal circularly polarized series-fed microstrip antenna array design," *IEEE Transactions on Antennas and Propagation*, Vol. 68, No. 2, 873–881, 2020.
5. Castro, A. T. and S. K. Sharma, "Inkjet-printed wideband circularly polarized microstrip patch array antenna on a PET film flexible substrate material," *IEEE Antennas and Wireless Propagation Letters*, Vol. 17, No. 1, 176-179, 2018.
6. Yinusa, K. A., "A dual-band conformal antenna for gnss applications in small cylindrical structures," *IEEE Antennas and Wireless Propagation Letters*, Vol. 17, No. 6, 1056–1059, 2018.
7. Zhong, J., A. Kiourti, T. Sebastian, Y. Bayram, and J. L. Volakis, "Conformal load-bearing spiral antenna on conductive textile threads," *IEEE Antennas and Wireless Propagation Letters*, Vol. 16, 230–233, 2017.
8. Jilani, S. F., M. O. Munoz, Q. H. Abbasi, and A. Alomainy, "Millimeter-wave liquid crystal polymer based conformal antenna array for 5G applications," *IEEE Antennas and Wireless Propagation Letters*, Vol. 18, No. 1, 84–88, 2019.
9. Yang, Z. K., N. Kou, S. X. Yu, Z. Ding, and Z. P. Zhang, "A coplanar waveguide-fed broadband circularly polarized microstrip antenna for conformal applications," *International Journal of RF and Microwave Computer-Aided Engineering*, Vol. 31, e22545, 2021.
10. Yang, H., Y. Fan, and X. Liu, "A compact dual-band stacked patch antenna with dual circular polarizations for beidou navigation satellite systems," *IEEE Antennas and Wireless Propagation Letters*, Vol. 18, No. 7, 1472–1476, 2019.

11. Wu, Q., X. Zhang, and L. Zhu, "Co-design of a wideband circularly polarized filtering patch antenna with three minima in axial ratio response," *IEEE Transactions on Antennas and Propagation*, Vol. 66, No. 10, 5022–5030, 2018.
12. Wu, Q., X. Zhang, and L. Zhu, "A feeding technique for wideband CP patch antenna based on 90° phase difference between tapped line and parallel coupled line," *IEEE Antennas and Wireless Propagation Letters*, Vol. 18, No. 7, 1468–1471, 2019.